

# HGCH: A Hyperbolic Graph Convolution Network Model for Heterogeneous Collaborative Graph Recommendation

Lu Zhang

luzhang\_cs@hust.edu.cn

Huazhong University of Science and Technology  
Wuhan, China

Ning Wu\*

wuning@buaa.edu.cn

Beihang University  
Beijing, China

## Abstract

User-item interaction data in collaborative filtering and graph modeling tasks often exhibit power-law characteristics, which suggest the suitability of hyperbolic space modeling. Hyperbolic Graph Convolution Neural Networks (HGCHNs) are a novel technique that leverages the advantages of GCN and hyperbolic space, and then achieves remarkable results. However, existing HGCHN methods have several drawbacks: they fail to fully leverage hyperbolic space properties due to arbitrary embedding initialization and imprecise tangent space aggregation; they overlook auxiliary information that could enrich the collaborative graph; and their training convergence is slow due to margin ranking loss and random negative sampling. To overcome these challenges, we propose Hyperbolic Graph Collaborative for Heterogeneous Recommendation (HGCH), an enhanced HGCHN-based model for collaborative filtering that integrates diverse side information into a heterogeneous collaborative graph and improves training convergence speed. HGCH first preserves the long-tailed nature of the graph by initializing node embeddings with power law prior; then it aggregates neighbors in hyperbolic space using the gyromidpoint method for accurate computation; finally, it fuses multiple embeddings from different hyperbolic spaces by the gate fusion with prior. Moreover, HGCH employs a hyperbolic user-specific negative sampling to speed up convergence. We evaluate HGCH on four real datasets, and the results show that HGCH achieves competitive results and outperforms leading baselines, including HGCHNs. Extensive ablation studies further confirm its effectiveness.

## CCS Concepts

• Information systems → Recommender systems; Collaborative filtering; • Computing methodologies → Neural networks.

## Keywords

Recommender Systems; Hyperbolic Embeddings; Graph Convolution

\*Corresponding Author

Permission to make digital or hard copies of all or part of this work for personal or classroom use is granted without fee provided that copies are not made or distributed for profit or commercial advantage and that copies bear this notice and the full citation on the first page. Copyrights for components of this work owned by others than the author(s) must be honored. Abstracting with credit is permitted. To copy otherwise, or to publish, to post on servers or to redistribute to lists, requires prior specific permission and/or a fee. Request permissions from [permissions@acm.org](https://doi.org/10.1145/3627673.3679701).

CIKM '24, October 21–25, 2024, Boise, ID, USA

© 2024 Copyright held by the owner/author(s). Publication rights licensed to ACM.

ACM ISBN 979-8-4007-0436-9/24/10

<https://doi.org/10.1145/3627673.3679701>

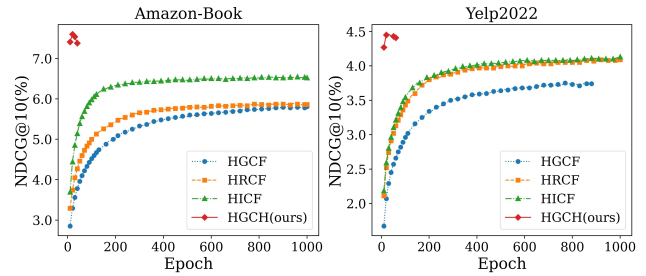


**Figure 1: NDCG@10 changes with training epochs on validation set of Amazon-Book and Yelp2022. Other metric@Ks show a similar tendency. HGCH converges very fast so only 40 and 60 epochs were trained on Amazon-Book and Yelp2022, respectively.**

## ACM Reference Format:

Lu Zhang and Ning Wu. 2024. HGCH: A Hyperbolic Graph Convolution Network Model for Heterogeneous Collaborative Graph Recommendation. In *Proceedings of the 33rd ACM International Conference on Information and Knowledge Management (CIKM '24)*, October 21–25, 2024, Boise, ID, USA. ACM, New York, NY, USA, 14 pages. <https://doi.org/10.1145/3627673.3679701>

## 1 Introduction

Recommender systems play a vital role in addressing information overload by offering personalized services to users and enhancing business revenue. One of the core methods employed in these systems is Collaborative Filtering (CF), which predicts user preferences based on historical user-item interactions. CF has been a focal point of research, leading to significant advancements.

Recent CF approaches leverage hyperbolic space, effectively capturing the power-law distribution and hierarchical structure in user-item interaction data. Prior studies [1, 27, 30] have revealed that such data often exhibit a tree-like structure, where the number of child nodes grows exponentially with distance from the root. This structure is distorted when modeled in Euclidean space, which has a polynomial growth of space capacity. In contrast, hyperbolic space, with its negative curvature, supports exponential growth of space capacity, making it an ideal fit for modeling tree-like data. Recent works on hyperbolic space-based recommender systems have shown promising results [9, 26, 37, 38, 51], particularly with Hyperbolic Graph Convolution Neural Networks (HGCHNs) [33, 48, 49], which combine the advantages of Graph Convolution Neural Networks (GCN) and hyperbolic space.

However, these works suffer from three shortcomings:

- The designs of these models only partially utilize the nature of hyperbolic space. This is mainly reflected in the following two

points: 1) node representations are initialized uniformly [33, 48, 49], ignoring the different levels of nodes in hyperbolic space; and 2) they utilize the tangent space at the origin to approximate neighbor aggregation, which introduces distortions in relative distances [4], potentially leading to suboptimal performance.

- Most works [33, 39, 49] use a combination of margin ranking loss and uniform random negative sampling, which leads to many invalid triplets in the late training period, resulting in optimization difficulties and slow convergence.
- They only consider user-item interaction data and neglect other types of side information that can enrich the collaborative graph. Although some works [14, 21, 32] incorporate side information into a heterogeneous graph, they still fail to capture the intrinsic characteristics of each sub-graph.

To address these challenges, we develop a novel HGCN model for CF with multiple side information, named **Hyperbolic Graph Collaborative for Heterogeneous Recommendation (HGCH)**. As shown in Fig. 1, HGCH converges significantly faster and performs better than previous methods. This improvement can be attributed to several important novelties: 1) power law prior-based initialization, which leverages the heterogeneous structure of hyperbolic space and facilitates better training results; 2) hyperbolic neighbor aggregation, which achieves more accurate computation results than tangent space neighbor aggregation; 3) gate fusion with prior, which effectively integrates different side information through prior-based training; 4) and hyperbolic user-specific negative sampling, which facilitates the sampling of a more valid training triplet. Moreover, our model only adds a small number of parameters compared to the state-of-the-art baseline, which further demonstrates the efficiency of our method. The main contributions of this work are summarized as follows:

- We propose a new method HGCH, which incorporates power law prior-based initialization, hyperbolic neighbor aggregation and gate fusion with prior to obtain a better distribution of node representations, thus enhancing the utilization of hyperbolic space (*i.e.*, leveraging its exponentially growing capacity to focus more on tail items).
- We found that the current combination of margin ranking loss and uniform random negative sampling limits the convergence speed of hyperbolic models. To address this, we propose a hyperbolic user-specific negative sampling method, which significantly accelerates the convergence speed of our HGCH compared to other hyperbolic methods. It should be noted that the proposed method is not limited to CF-based models, but is also applicable to other hyperbolic recommendation models.
- Extensive experiments demonstrate the effectiveness of the proposed method where the maximum recommendation effect on overall items versus all baselines is up to 22.49%. Our source code is available here: <https://github.com/LukeZane118/HGCH>.

## 2 Related Work

In this section, we review related work from the GCN to HGCN.

### 2.1 Graph Convolution Neural Networks

GCN-based methods have received much attention due to their ability to learn node representations from arbitrary graph structures

[28, 44]. They are widely used in the fields of computer vision [22, 45, 47], natural language processing [3, 25, 44], and biocomputing [8, 10, 19]. There are also some representative GCN approaches in the field of recommender systems. NGCF [41] generalizes GCN to the domain of recommender systems. While LightGCN [13] further exposes that feature transformations and nonlinear activations in GCN do not play a role in recommendation tasks and thus can be removed. DGCF [42], on the other hand, attempts to model the user’s intent using GCN. However, these approaches are mainly built in Euclidean space, which may underestimate the distribution of the user-item dataset. Recent work [4, 23, 52] has demonstrated the potent power of hyperbolic space to model graph-structured data with hierarchical and power-law distributions.

### 2.2 Hyperbolic Recommender Systems

Hyperbolic recommender systems have been receiving more and more attention lately. HyperML [37] bridges the gap between Euclidean and hyperbolic geometry in recommender systems for the representation of the user and the item through metric learning methods. HAE and HVAE [26] generalize AE and VAE to hyperbolic space for implicit recommendation, respectively. HSCML [51] proposes hyperbolic social collaboration metric learning by driving socially relevant users closer to each other. HME [9] applies hyperbolic space to the point-of-interest recommendation and introduces various side information such as sequential transition, user preference, category, and region information. HyperSoRc [38] learns the representation of users and items in hyperbolic space by introducing social information. However, these methods lack the utilization of higher-order connection information of nodes.

Combining graph neural networks, LKGR [6] introduces a knowledge-aware attention mechanism for hyperbolic recommender systems. HGCF [33] implements multiple layers of skip-connected graph convolutions through tangent spaces to capture high-order connectivity information between nodes. Based on HGCF, HRCF [49] designs a geometry-aware hyperbolic regularizer to facilitate the optimization process. Furthermore, HICF [48] proposes an adaptive hyperbolic margin ranking loss. Also based on HGCF, LGCF [39] uses the midpoint of hyperbolic space to realize neighbor aggregation instead of tangent space. However, the designs of these HGCN-based methods do not take full advantage of the nature of hyperbolic space, *i.e.*, simplistic embedding initialization approach and neighbor aggregation by tangent space at the origin.

Furthermore, it should be noted that although LGCF also employs the midpoint in hyperbolic space instead of the tangent space for neighbor aggregation, it involves a transformation process from the Lorentz model to the Klein model [39]. Whether the Einstein midpoint in the Klein model has a geometric interpretation in the Lorentz model remains to be studied [5]. Moreover, issues regarding the fairness and validity of the experiments conducted in this work have been pointed out.<sup>1</sup> In contrast, our approach utilizes the gyromidpoint of the Poincaré model, which allows us to compute the generalized mean of points in hyperbolic space without the need for further conversion to other hyperbolic models. Another similar work is HICF, which proposes a sampling method in hyperbolic space for sampling negative items closer to the positive item,

<sup>1</sup>Relevant details can be found in the note of <https://github.com/marlin-codes/HRCF>.

providing additional information for optimization. In contrast, our method samples negative items in hyperbolic space nearer to the user, generating more valid triplets to speed up convergence.

### 3 Preliminaries

In this section, we first introduce the hyperbolic space approach relevant to this paper and then present our task description.

#### 3.1 Hyperbolic Space

Our goal is to learn low-dimensional embeddings in hyperbolic space, which better capture hierarchical structures than Euclidean space. We use the Poincaré model of hyperbolic geometry, which facilitates computing generalized means of points in hyperbolic space [36]. In a  $d$ -dimensional hyperbolic space with curvature  $c$  (a negative constant), the negative reciprocal is  $k = -1/c$  (non-negative). A hyperbolic space is a Riemannian manifold where the metric depends on the curvature. The tangent space  $\mathcal{T}_x\mathcal{M}$  at a point  $x$  on the manifold  $\mathcal{M}$  is a  $d$ -dimensional Euclidean space approximating the manifold locally at  $x$ . The Poincaré model, which is mathematically equivalent to other hyperbolic space representations, is defined by:

$$\mathcal{B}^d := \{x \in \mathbb{R}^d \mid \|x\|^2 < k\}, \quad (1)$$

where  $\|\cdot\|$  denotes the Euclidean norm. The distance in the Poincaré model is given by:

$$d_{\mathcal{B}}(x, y) = \sqrt{k} \operatorname{arccosh} \left( 1 + 2k \frac{\|x - y\|^2}{(k - \|x\|^2)(k - \|y\|^2)} \right). \quad (2)$$

To generalize the operations of Euclidean space to hyperbolic space, we can use the tangent space  $\mathcal{T}_x\mathcal{M}$  as an approximation. The exponential mapping  $\exp_x^k$  and the logarithmic mapping  $\log_x^k$  enable the transformation between the tangent space and the hyperbolic space. We fix the origin  $\mathbf{o} = (0, 0, \dots, 0) \in \mathcal{B}^d$  and use it as a reference point throughout this paper. In the Poincaré method, the exponential mapping  $\exp_{\mathbf{o}}^k: \mathcal{T}_{\mathbf{o}}\mathcal{B}^d \rightarrow \mathcal{B}^d$  is defined as [36]:

$$\exp_{\mathbf{o}}^k(v) = \tanh\left(\frac{\|v\|}{\sqrt{k}}\right) \frac{\sqrt{k}v}{\|v\|}, \quad (3)$$

the logarithmic mapping  $\log_{\mathbf{o}}^k: \mathcal{B}^d \rightarrow \mathcal{T}_{\mathbf{o}}\mathcal{B}^d$  is given by [36]:

$$\log_{\mathbf{o}}^k(y) = \operatorname{arctanh}\left(\frac{\|y\|}{\sqrt{k}}\right) \frac{\sqrt{k}y}{\|y\|}. \quad (4)$$

#### 3.2 Task Formulation

In this section, we present the key concepts and notations used in our work, such as Heterogeneous Collaborative Graph (HCG), high-order node connectivity, and compositional edge relations.

**3.2.1 User-Item Bipartite Graphs.** A common way to represent the historical interactions between users and items (e.g., purchases and visits) in a recommender system is to use a user-item bipartite graph  $\mathcal{G}_0 = (\mathcal{U} \cup \mathcal{V}, \mathcal{E}_0)$ , where  $\mathcal{U}$  and  $\mathcal{V}$  denote the user set and item set, respectively, and an edge  $y_{u,v} = 1$  in edge set  $\mathcal{E}_0$  indicates that user  $u$  has interacted with item  $v$ ; otherwise  $y_{u,v} = 0$ .

**3.2.2 Heterogeneous Collaborative Graph.** We define a heterogeneous collaborative graph as  $\mathcal{G} = \mathcal{G}_0 \cup \mathcal{G}' = (\mathcal{H}, \mathcal{E})$ , where  $\mathcal{H}$  is the node set that includes user nodes  $\mathcal{U}$ , item nodes  $\mathcal{V}$  and other optional nodes such as category nodes etc.  $\mathcal{E}$  is the edge set

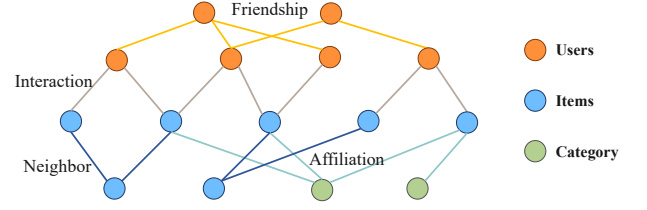


**Figure 2: An Example of a Heterogeneous Collaborative Graph. Its node set contains the user, item, and category; its edge set contains the user-item link, user-user link, item-item link and item-category link.**

that includes user-item edges  $\mathcal{E}_0$  and other types of edges, and  $\mathcal{G}' = \{\mathcal{G}_1, \mathcal{G}_2, \dots, \mathcal{G}_{|\mathcal{S}|-1}\}$  represents the set of all side-information graphs. A heterogeneous collaborative graph  $\mathcal{G}$  is also associated with a node type mapping function  $\phi: \mathcal{H} \rightarrow \mathcal{T}$  and an edge type mapping function  $\psi: \mathcal{E} \rightarrow \mathcal{S}$ .  $\mathcal{T}$  and  $\mathcal{S}$  denote predefined node types and edge types, respectively, where  $|\mathcal{T}| + |\mathcal{S}| > 2$ . Fig. 2 shows an example of the HCG.

**3.2.3 Problem Statement.** Based on the above definitions, we can formulate the recommendation problem that we aim to address in this paper as follows:

- **Input:** a heterogeneous collaborative graph  $\mathcal{G}$  comprising a user-item interaction graph  $\mathcal{G}_0$  and a side information subgraph  $\mathcal{G}'$ .
- **Output:** a function that estimates the probability  $\hat{y}_{u,v}$  of user  $u$  accepting item  $v$ .

## 4 Method

We now propose the HGCH model, which leverages hyperbolic geometry to capture complex and hierarchical relationships in recommender systems. The model consists of three main components, as illustrated in Fig. 3: 1) a power law prior-based embedding layer initializing nodes in tangent space by popularity; 2) a hyperbolic aggregation and fusion layer updating node embeddings through prior-based gating; and 3) a prediction layer that computes matching scores between nodes in the hyperbolic space. In addition, our HGCH also includes a hyperbolic user-specific negative sampling for accelerating the training convergence speed.

### 4.1 Embedding Layer with Power Law Prior

Most existing hyperbolic recommender systems define node embeddings in the hyperbolic space and train them with a Riemannian optimizer [9, 33, 48, 49]. However, as reported by AMCAD [46] and confirmed by our initial experiments, this approach does not offer significant advantages over defining and training node embeddings in the tangent space (Euclidean space) with a Euclidean optimizer. Therefore, we adopt the latter approach in our model. The initialization of node embeddings is crucial for the optimization process and the final performance [11]. A good initialization should reflect the inherent properties of the data, while a bad initialization may lead to suboptimal solutions. Previous works [9, 33, 48, 49] initialized node embeddings by sampling from uniform or Gaussian distributions in the tangent space. However, this ignores the fact that node

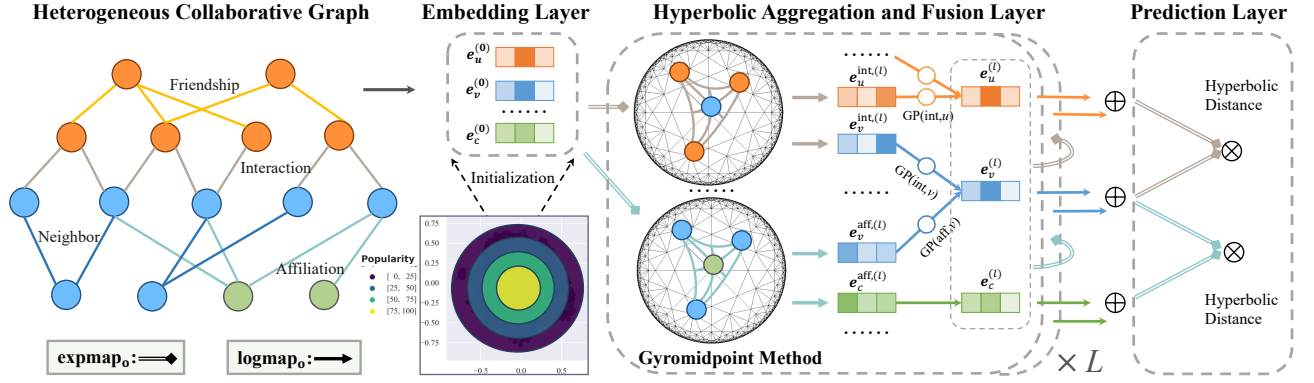


**Figure 3: An illustration of HGCH model architecture. It consists of three main components: 1) power law prior-based embedding layer, 2) hyperbolic aggregation and fusion layer, and 3) prediction layer. Note that "int" and "aff" denote the subspace "interaction" and "affiliation", respectively. "GP" means gate fusion with prior.**

popularity is correlated with the norm of the hyperbolic embedding, such that more popular nodes tend to have smaller norms and are closer to the origin [9, 33]. A uniform or Gaussian prior distribution for all nodes probably results in misplacing popular nodes far from the origin, which may hamper the model's ability to learn meaningful representations.

To address this issue, we propose to initialize node embeddings based on a power law prior distribution, which assigns different initialization ranges to nodes according to their popularity. In this way, nodes with higher popularity are more likely to be initialized near the origin, while nodes with lower popularity are more likely to be initialized away from the origin. Formally, given a uniform distribution, the power law prior-based sampling distribution of node  $n$  is:

$$\mathbf{e}_n^{(0)} \sim \text{Uni}(-ax_n^{-b}, ax_n^{-b}), \quad (5)$$

where  $x_n$  denotes the frequency of node  $n$ ,  $a$  is the scale of initialization consistent with uniform initialization, and  $b$  is the hyperparameter of power law distribution. Note that since  $\exp_o^k$  and  $\log_o^k$  are both conformal [36], the prior distribution is preserved when mapping embeddings between tangent and hyperbolic spaces.

## 4.2 Hyperbolic Aggregation and Fusion Layers

Next, we establish a novel hyperbolic graph convolution layer that recursively propagates and fuses embeddings from different subspaces through high-order connectivity. In this section, we first introduce the two components of our layer: hyperbolic neighbor aggregation and gate fusion with prior. Then we explain how to stack multiple layers for deeper representation learning.

**4.2.1 Hyperbolic Neighbor Aggregation.** Previous work [4] extends the Euclidean GCN neighbor aggregation to hyperbolic space by the tangent space method. It consists of three steps: 1) project the hyperbolic space embedding to the tangent space at the origin by  $\log_o^k$ ; 2) apply the Euclidean GCN neighbor aggregation in the tangent space; and 3) project the embedding back to the hyperbolic space by  $\exp_o^k$ . In this way, the GCN neighbor aggregation in hyperbolic space can be approximated. Formally, given a hyperbolic space embedding of node  $n$ , its tangent space neighbor aggregation

proceeds according to the following equations:

$$\mathbf{e}_n^{(l-1)} = \log_o^k(\mathbf{h}_n^{(l-1)}), \quad (6)$$

$$\mathbf{e}_n^{(l)} = \sum_{i \in \mathcal{N}_n} \frac{1}{|\mathcal{N}_n|} \mathbf{e}_i^{(l-1)}, \quad (7)$$

$$\mathbf{h}_n^{(l)} = \exp_o^k(\mathbf{e}_n^{(l)}), \quad (8)$$

where  $\mathcal{N}_n$  denotes the set containing node  $n$  itself and its neighbors. However, this approach has such a drawback: it performs neighbor aggregation of all nodes in the same tangent space (the origin), instead of their own tangent spaces, which introduces distortions in relative distance [4], thus may lead to a suboptimal recommendation effect. To address this issue, we propose to directly implement neighbor aggregation in hyperbolic space using the gyromidpoint method [36], which computes the weighted average of a set of points in hyperbolic space as follows:

$$m(\mathbf{x}_1, \dots, \mathbf{x}_N; \mathbf{v}) = \frac{1}{2} \otimes_k \left[ \sum_{i=1}^N \frac{v_i \lambda(k, \mathbf{x}_i)}{\sum_{j=1}^N v_j (\lambda(k, \mathbf{x}_j) - 1)} \mathbf{x}_i \right], \quad (9)$$

where  $v_i$  is the weight of node  $\mathbf{x}_i$ ,  $\lambda(k, \mathbf{x}) = 2 \left(1 - \frac{\|\mathbf{x}\|^2}{k}\right)^{-1}$  ( $\|\cdot\|$  is Euclidean norm), and  $\otimes_k$  is the Möbius scalar multiplication [36]. For simplicity, we set  $v_i$  to 1 for all nodes, meaning that they have equal importance. Other methods, such as attention mechanism [2], can be used to learn different weights for different nodes, but this is beyond the scope of this paper. The gyromidpoint method is a natural generalization of the Euclidean midpoint to hyperbolic space. It preserves the distance between points and their midpoint, and it is invariant under isometries of hyperbolic space. So it can be seen as a way of performing neighbor aggregation in hyperbolic space by averaging the information from neighboring nodes.

Hence, given the tangent space embedding of a node  $n$  of  $(l-1)$ -th layer, we want to get the neighbor information of  $n$  from subgraph  $\mathcal{G}'$ . We first project it into the hyperbolic subspace  $s$  by  $\exp_o^k$ :

$$\mathbf{h}_n^{s, (l-1)} = \exp_o^{k_s}(\mathbf{e}_n^{(l-1)}). \quad (10)$$

The exponential map  $\exp_{\mathbf{o}}^k$  maps a point in the tangent space at the origin  $\mathbf{o}$  to a point in hyperbolic space with curvature  $k$ . It preserves the distance and angle between vectors in the tangent space and their images in hyperbolic space. It can be seen as a way of projecting information from Euclidean space to hyperbolic space by preserving the geometry. Then we perform neighbor aggregation by Eq. (9):

$$\mathbf{h}_n^{s,(l)} = \frac{1}{2} \otimes_{k_s} \left[ \sum_{i \in \mathcal{N}_n} \frac{\lambda(k_s, \mathbf{h}_i^{s,(l-1)})}{\sum_{j \in \mathcal{N}_n} (\lambda(k_s, \mathbf{h}_j^{s,(l-1)}) - 1)} \mathbf{h}_n^{s,(l-1)} \right], \quad (11)$$

thus aggregating information from neighboring nodes directly in hyperbolic space.

**4.2.2 Multi-Space Information Fusion.** After neighbor aggregation in each subspace, we need to fuse the output from each subspace to update the embedding of the nodes. Since the curvature of each subspace is not necessarily the same, we need to project the embedding to a uniform tangent space first, as follows:

$$\mathbf{e}_n^{s,(l)} = \log_{\mathbf{o}}^{k_s}(\mathbf{h}_n^{s,(l)}). \quad (12)$$

Then we can consider the fusion of multiple information in the tangent space, which is:

$$\mathbf{e}_n^{(l)} = \sum_{s \in \mathcal{S}_n} \mathbf{g}_n^s \odot \mathbf{e}_n^{s,(l)}, \quad (13)$$

where  $\mathcal{S}_n$  is the set of subspaces that node  $n$  involves in,  $\odot$  is element-wise product and  $\mathbf{g}_n^s$  is the weight of embedding  $\mathbf{e}_n^s$ . An intuitive idea is to set a learnable weight to control the weight of each kind of information automatically. Accordingly, we use the gate mechanism to implement this idea, which we call gate fusion. It is formulated as follows:

$$\mathbf{g}_{\text{gate}} = \frac{\sigma(\mathbf{W}_{t_n}^s \mathbf{e}_n^{(0)} / \|\mathbf{e}_n^{(0)}\|)}{\sum_{i \in \mathcal{S}_n} \sigma(\mathbf{W}_{t_n}^i \mathbf{e}_n^{(0)} / \|\mathbf{e}_n^{(0)}\|)}, \quad (14)$$

where  $t_n$  is the type of node  $n$ , i.e.,  $t_n \in \{user, item, category, \dots\}$ ,  $\mathbf{W}_{t_n}^s$  is the learnable parameter of the gate of subspace  $s$  corresponding to the type of node  $n$ , and  $\sigma$  is the sigmoid function. The gate mechanism is a way of learning adaptive weights for different kinds of information based on their relevance to the node type and their initial embedding. The sigmoid function ensures that the weights are between 0 and 1, and normalized by their sum. The gate mechanism can help select useful information and filter out noisy information for each node type. However, in practice, we found that gate fusion can easily fall into the local optimum and even perform less well than the model without side information in some cases. So we directly use normalized neighbor numbers of node  $n$  in subspace  $s$  as a prior weight, namely prior-based fusion, and it is given by:

$$\mathbf{g}_{\text{prior}} = \frac{|\mathcal{N}_n^s|}{\sum_{i \in \mathcal{S}_n} |\mathcal{N}_n^i|}. \quad (15)$$

The prior-based fusion is a way of assigning weights for different kinds of information based on their frequency or density in each subspace. The intuition is that more neighbors imply more information and thus higher importance. The prior-based fusion can

help balance different kinds of information and avoid overfitting or underfitting problems. What is more, if the gate fusion can learn based on prior instead of learning from scratch, the performance may get further improvement. Therefore, we combine the two and call this approach the gate fusion with prior, which is defined as:

$$\mathbf{g}_{\text{gate\&prior}} = \frac{|\mathcal{N}_n^s| \sigma(\mathbf{W}_{t_n}^s \mathbf{e}_n^{(0)} / \|\mathbf{e}_n^{(0)}\|)}{\sum_{i \in \mathcal{S}_n} |\mathcal{N}_n^i| \sigma(\mathbf{W}_{t_n}^i \mathbf{e}_n^{(0)} / \|\mathbf{e}_n^{(0)}\|)}. \quad (16)$$

According to experiments, gate fusion with prior is better and stable in most cases, so we adopt this structure for HGCH. The empirical comparison of these structures is shown in Section 6.5. Although we avoid the distortion of neighbor aggregation, we still inevitably bring distortion when introducing side information since it is difficult to directly aggregate nodes in different hyperbolic spaces with different curvatures. However, it is confirmed by Section 6.5 that the benefits of introducing side information far outweigh the drawback. Besides, we also use the learnable gate method as a remedy for the distortion. If both neighbor aggregation and information fusion are implemented in tangent space, two distortions will be accumulated.

**4.2.3 High-Order Propagation.** Further, we can stack multiple layers to explore high-order connectivity information and collect information from multi-hop neighbors. However, previous work [33] found that stacking multiple layers leads to degradation in the model's overall performance due to gradient disappearance and over smoothing. Here, we refer to HGCF [33] and use SkipGCN to aggregate the output of multiple layers, which is defined as follows:

$$\mathbf{e}_n = \sum_{i=1}^L \mathbf{e}_n^{(i)}, \quad (17)$$

where  $L$  is the number of convolutional layers. The SkipGCN is a way of combining information from all layers by adding skip connections from each layer to the final layer. The skip connections can help preserve the original information and avoid the loss of gradient and information during the propagation process. In this way, the final output of the convolutional layer embedding contains rich neighbor information and side information, and we next employ the hyperbolic distance  $d_{\mathcal{B}}$  to evaluate the similarity of node pairs.

### 4.3 Prediction Layer

The embeddings of the final output are first projected into the hyperbolic space of the scoring layer, and then we use the hyperbolic distance  $d_{\mathcal{B}}$  defined in Eq. (2) to measure the similarity of the projected embeddings  $\mathbf{h}_i$  and  $\mathbf{h}_j$ , as follows:

$$\mathbf{h}_i = \exp_{\mathbf{o}}^{k_s}(\mathbf{e}_i), \quad (18)$$

$$\mathbf{h}_j = \exp_{\mathbf{o}}^{k_s}(\mathbf{e}_j), \quad (19)$$

$$\hat{y}_{i,j} = -d_{\mathcal{B}}(\mathbf{h}_i, \mathbf{h}_j)^2. \quad (20)$$

The hyperbolic distance  $d_{\mathcal{B}}$  is based on the inner product of two points in hyperbolic space. It reflects the similarity between two nodes based on their hyperbolic embeddings. This completes the prediction of the node pair ratings.

**Algorithm 1** Hyperbolic User-specific Negative Sampling

**Input:** Hyperparameters  $n_{\text{neg}}$ ; The item set  $\mathcal{V}$ ; The embedding matrix  $\mathbf{E}$ ; The index of the user  $u$  and his/her positive item  $\mathcal{V}_u$  in the training set.

**Output:** The item index of the negative sample.

```

1:  $\mathcal{V}_u^{\text{neg}} \leftarrow$  randomly sample  $n_{\text{neg}}$  items from  $\mathcal{V} \setminus \mathcal{V}_u$ 
2:  $\text{minDist} \leftarrow \infty$ 
3:  $\text{minIndex} \leftarrow -1$ 
4: Get the tangent embeddings of  $u$  the from  $\mathbf{E}$ , i.e.  $\mathbf{e}_u$ 
5:  $\mathbf{h}_u \leftarrow \exp_0^k(\mathbf{e}_u)$ 
6: for  $i \in \mathcal{V}_u^{\text{neg}}$  do
7:   Get the tangent embeddings of  $i$  the from  $\mathbf{E}$ , i.e.  $\mathbf{e}_i$ 
8:    $\mathbf{h}_i \leftarrow \exp_0^k(\mathbf{e}_i)$ 
9:    $d_{u,i} \leftarrow d_{\mathcal{B}}(\mathbf{h}_u, \mathbf{h}_i)$ 
10:  if  $d_{u,i} < \text{minDist}$  then
11:     $\text{minDist} \leftarrow d_{u,i}$ 
12:     $\text{minIndex} \leftarrow i$ 
13:  end if
14: end for
15: return  $\text{minIndex}$ 

```

#### 4.4 Optimization

We adopt the margin ranking loss used by HGCF [33] to optimize our model. The margin ranking loss for the target subgraph  $\mathcal{G}_0$  is given by:

$$\mathcal{L}_{\text{CF}} = \mathcal{L}_{\mathcal{G}_0} = \max(\hat{y}_{u,j} - \hat{y}_{u,i} + m, 0), \quad (21)$$

where  $m$  is a margin parameter, item  $i$  is a positive sample drawn from  $y_{u,i} = 1 \in \mathcal{G}_0$ , and item  $j$  is a negative sample drawn from  $\mathcal{V}$ . The margin  $m$  specifies the minimum difference required between positive and negative sample scores. As  $m$  approaches infinity, the margin ranking loss becomes equivalent to the BPR Loss [31]. However, this causes the model to focus too much on easy pairs, resulting in slow training and poor performance due to many embeddings clustering near the boundaries of the ball space. For other subgraphs  $\mathcal{G}'$ , we also train their embeddings by margin ranking loss:

$$\mathcal{L}_{\text{SI}} = \sum_{\mathcal{G}_i \in \mathcal{G}'} \mathcal{L}_{\mathcal{G}_i}, \quad (22)$$

where node  $\mathcal{G}_i$  denotes subgraphs of each link type, and we only sample negative nodes in subgraph  $\mathcal{G}_i$  when calculating  $\mathcal{L}_{\mathcal{G}_i}$ . Eventually, our objective function is a multitask loss with  $\mathcal{L}_{\text{CF}}$  as the main task and  $\mathcal{L}_{\text{SI}}$  as the auxiliary task:

$$\mathcal{L} = \mathcal{L}_{\text{CF}} + \alpha \mathcal{L}_{\text{SI}}, \quad (23)$$

where  $\alpha$  is the hyperparameter that controls the weight of the auxiliary task  $\mathcal{L}_{\text{SI}}$ .

Moreover, in our preliminary experiments, we observed that HGCH-based methods tend to converge slowly. This phenomenon is likely due to the inefficiency of random sampling techniques for sampling training triplets in this setting. It is easy to see that, during the later stages of training, most negative pairs  $(u, j)$  and positive pairs  $(u, i)$  already have a distance larger than the margin  $m$ , making them ineffective for optimization. Furthermore, random

sampling assumes a uniform distribution, which treats all items equally, leading to most sampled training triplets being invalid for model optimization. To address this issue, we need a user-specific, self-optimizing, and data-independent method. Alg. 1 shows our approach. In each iteration, we randomly pick  $n_{\text{neg}}$  items  $\mathcal{V}_u^{\text{neg}}$  and compute their hyperbolic distances to user  $u$ . Then, we keep the item with the smallest distance, which means it is close to user  $u$  in the hyperbolic space. This strategy guarantees that the sampled negative node remains close to user  $u$ , thereby facilitating the sampling of valid training triplets.

## 5 Discussion

### 5.1 Space Complexity Analysis

HGCH's space complexity has two main parts: 1) node embedding,  $O(|\mathcal{H}|d)$ ; and 2) gate,  $O(|\mathcal{G}|d^2)$ . Hence the total space complexity is  $O((|\mathcal{H}| + |\mathcal{G}|d)d)$ . When only using user-item interaction data, the space complexity of HGCH is  $O(|\mathcal{H}|d)$ , which is consistent with the lightweight models having only embedding parameters such as LightGCN [13] and HGCF [33]; when including side information, the numbers of new node from side graph are generally small in real scenarios. Besides, it is often  $|\mathcal{H}| \gg |\mathcal{G}|d$ , so HGCH only adds a small number of parameters in this case.

### 5.2 Relation to Heterogeneous Graph Methods

Heterogeneous graph recommendations often use path-based methods, which extract high-order path information for the model. They either select salient paths [35, 43] or use predefined meta-paths [15, 18, 34, 50] to handle multiple node relationships. However, the paths are not optimized for the recommendation goals, or they need domain knowledge and may not be optimal. Traditional methods struggle with large and complex nodes and relations [40]. Our approach separately processes and fuses different node relationships by hyperbolic subspace and multi-space information fusion, and then combines multiple relationship paths by multi-layer GCN's high-order connectivity.

## 6 Experiments

We evaluate our proposed approach on four real data sets. We want to answer the following research questions:

- **RQ1:** How does HGCH perform compared to the state-of-the-art recommender methods?
- **RQ2:** What is the impact of each component?
- **RQ3:** How well do different fusion methods work on HGCH?
- **RQ4:** What kind of embedding has HGCH method learned?
- **RQ5:** How about the convergent speed of HGCH?

### 6.1 Dataset Description

We evaluate the proposed method on four public available datasets: Amazon-CD<sup>2</sup>, Amazon-Book<sup>2</sup>, Gowalla<sup>3</sup>, and Yelp2022<sup>4</sup>, each varying in domain, size, sparsity, and side information. We had to process the raw data from scratch to include side information, as previous studies [13, 41] only offered processed interaction datasets.

<sup>2</sup><http://jmcauley.ucsd.edu/data/amazon>.

<sup>3</sup><http://snap.stanford.edu/data/loc-gowalla.html>.

<sup>4</sup><https://www.yelp.com/dataset>.

**Table 1: Performances for all datasets. The best performing model on each dataset and metric is highlighted in bold, and second best model is underlined. Asterisks denote statistically significant wilcoxon signed rank test for the difference in scores between the best and second-best models.**

Datasets	Metric	BPRMF	WRMF	NGCF	LightGCN	DGCF	HGCF	HRCF	HICF	HGCH	HGCF+	HRCF+	HICF+	HGCH+	$\Delta$ (%)	$\Delta_+$ (%)
Amazon-CD	R@10	0.0666	0.0762	0.0710	0.0834	0.0765	0.0975	0.1015	<u>0.1031</u>	<b>0.1067*</b>	0.1055	0.0983	0.1009	<b>0.1196*</b>	3.49%	16.00%
	R@20	0.1036	0.1147	0.1092	0.1259	0.1138	0.1436	0.1476	<u>0.1522</u>	<b>0.1555*</b>	0.1585	0.1483	0.1518	<b>0.1743*</b>	2.17%	14.52%
	N@10	0.0553	0.0631	0.0586	0.0688	0.0633	0.0823	0.0843	<u>0.0867</u>	<b>0.0904*</b>	0.0872	0.0798	0.0824	<b>0.1010*</b>	4.27%	16.49%
	N@20	0.0672	0.0756	0.0710	0.0825	0.0754	0.0969	0.0989	<u>0.1021</u>	<b>0.1057*</b>	0.1042	0.0960	0.0988	<b>0.1182*</b>	3.53%	15.77%
Amazon-Book	R@10	0.0666	0.0609	0.0637	0.0827	0.0714	0.0983	0.0996	<u>0.1099</u>	<b>0.1261*</b>	0.1008	0.0996	0.1115	<b>0.1320*</b>	14.74%	20.11%
	R@20	0.0998	0.0927	0.0974	0.1215	0.1069	0.1413	0.1434	<u>0.1553</u>	<b>0.1701*</b>	0.1451	0.1434	0.1577	<b>0.1797*</b>	9.53%	15.71%
	N@10	0.0537	0.0511	0.0523	0.0690	0.0591	0.0835	0.0843	<u>0.0947</u>	<b>0.1118*</b>	0.0845	0.0833	0.0953	<b>0.1160*</b>	18.06%	22.49%
	N@20	0.0645	0.0614	0.0632	0.0815	0.0706	0.0972	0.0984	<u>0.1090</u>	<b>0.1251*</b>	0.0987	0.0973	0.1099	<b>0.1305*</b>	14.77%	19.72%
Gowalla	R@10	0.1075	0.0999	0.1143	0.1286	0.1204	0.1296	0.1303	<u>0.1342</u>	<b>0.1447*</b>	0.1392	0.1409	0.1453	<b>0.1576*</b>	7.82%	17.44%
	R@20	0.1578	0.1499	0.1697	0.1853	0.1755	0.1912	0.1914	<u>0.1959</u>	<b>0.2086*</b>	0.2053	0.2061	0.2114	<b>0.2273*</b>	6.48%	16.03%
	N@10	0.0535	0.0926	0.1110	0.1262	0.1171	0.1237	0.1247	<u>0.1289</u>	<b>0.1396*</b>	0.1343	0.1351	0.1402	<b>0.1532*</b>	8.30%	18.85%
	N@20	0.1188	0.1093	0.1277	0.1432	0.1338	0.1420	0.1428	<u>0.1471</u>	<b>0.1581*</b>	0.1538	0.1546	0.1598	<b>0.1734*</b>	7.48%	17.88%
Yelp2022	R@10	0.0500	0.0629	0.0546	0.0655	0.0609	0.0667	0.0718	<u>0.0733</u>	<b>0.0790*</b>	0.0666	0.0657	0.0679	<b>0.0795*</b>	7.78%	8.46%
	R@20	0.0838	0.1017	0.0897	0.1057	0.0986	0.1109	0.1191	<u>0.1206</u>	<b>0.1273*</b>	0.1108	0.1099	0.1128	<b>0.1280*</b>	5.56%	6.14%
	N@10	0.0409	0.0514	0.0448	0.0552	0.0508	0.0549	0.0595	<u>0.0606</u>	<b>0.0660*</b>	0.0549	0.0538	0.0557	<b>0.0670*</b>	8.91%	10.56%
	N@20	0.0520	0.0642	0.0563	0.0682	0.0629	0.0693	0.0748	<u>0.0758</u>	<b>0.0814*</b>	0.0692	0.0681	0.0702	<b>0.0824*</b>	7.39%	8.71%

## 6.2 Experimental Settings

**6.2.1 Evaluation Metrics.** We adopt two widely-used evaluation metrics Recall@ $K$  and NDCG@ $K$  [17], with  $K$  set to 10 and 20. Our experiments are conducted on the RecBole [53] framework, following its implementation of Recall@ $K$  and NDCG@ $K$ .

**6.2.2 Baselines.** To show the effectiveness of our model, we compare our proposed HGCH with latent factor-based (BPRMF [31] and WRMF [16]), GCN-based (NGCF [41], LightGCN [13], and DGCF [42]), and HGCN-based (HGCF [33], HRCF [49], and HICF [48]). Besides, we refer to the version using HCG directly as HGCF+, HRCF+, and HICF+, respectively. For our model, we denote the version that uses only the user-item bipartite graph and the version that utilizes HCG as HGCH and HGCH+, respectively. Note that the main difference between HGCF+/HRCF+/HICF+ and HGCH+ is the neighbor aggregation, the former proceeds directly on the HCG, but the latter performs on each subgraph of the HCG separately.

We do not include LGCF [39] as it has been noted to have issues<sup>1</sup>. In addition, although there are more recent GCN-based methods [24, 29], we primarily focus on LightGCN, as it serves as the backbone for HGCF, HRCF, HICF, and our method. These newer GCN-based methods can be integrated with ours.

**6.2.3 Hyperparameter Settings.** We followed the original settings and tuned the parameters for each model. Compared to previous work that generally trained for 500 epochs [33, 48, 49], we extended the training to 1000 epochs because we found many methods had not yet converged. Additionally, consistent with prior work, we employed an early stopping strategy, meaning that training was stopped early if the NDCG@10 on the validation set did not improve for 100 consecutive epochs.

## 6.3 Performance Comparison (RQ1)

Table 1 shows the test set results, highlighting the best (bold), second-best (underline), and relative gains ( $\Delta$  and  $\Delta_+$ ) of HGCH and HGCH+ over the strongest baseline. From the table, we observe:

- HGCH outperforms all baselines when only interaction data is considered, with up to 18.06% improvement. Hyperbolic models, including HGCH, HGCF, HRCF, and HICF, have an edge over Euclidean models for modeling large user-item networks with power-law distributions. Among hyperbolic models, HGCH benefits more from data quantity. For example, HGCH improves more on larger datasets like Amazon-Book (+14.74% for Recall@10 and +18.06% for NDCG@10) than on Amazon-CD (+3.49% for Recall@10 and +4.27% for NDCG@10) compared to second-best HICF, indicating better use of hyperbolic space.
- The incorporation of side information into our model, resulting in HGCH+, yields further enhancements across all datasets. In contrast, other hyperbolic models' performance varies depending on the dataset; they sometimes exhibit significant improvements, while at other times their performance remains stagnant or even declines. A case in point is the Yelp2022 dataset, where other hyperbolic models incorporating side information suffer a considerable performance dip, while our HGCH+ maintains a modest improvement. This highlights the potential pitfalls of direct HCG usage, while validating HGCH's more effective utilization of side information.

## 6.4 Ablation Analysis (RQ2)

To further test our proposal, we evaluated how each HGCH component affects the performance. Table 2 show the results. Here, HS, PI, HA, and GP mean Hyperbolic negative Sampling, Power law prior-based Initialization, Hyperbolic neighbor Aggregation, and Gate fusion with Prior, respectively. Parentheses show the improvement over the first row (Base) of the table. Table 2 reveals that:

- Our HS enhances performance on each dataset (row 2 in Table 2), and this improvement is strongly correlated with the number of items in each dataset. The ranking of the improvements is consistent with the ranking of the number of items in each dataset.
- Coupling PI with HS results in further performance boosts across all datasets (row 5 in Table 2), especially for Amazon-Book, where

**Table 2: Evaluation of HGCH with different subsets of components for all datasets.**

Component				Amazon-CD				Amazon-Book			
HS	PI	HA	GP	Recall@10	Recall@20	NDCG@10	NDCG@20	Recall@10	Recall@20	NDCG@10	NDCG@20
				0.0930 (0.0%)	0.1375 (0.0%)	0.0785 (0.0%)	0.0926 (0.0%)	0.0921 (0.0%)	0.1304 (0.0%)	0.0797 (0.0%)	0.0919 (0.0%)
✓				0.0960 (3.2%)	0.1390 (1.1%)	0.0827 (5.4%)	0.0960 (3.7%)	0.1062 (15.3%)	0.1431 (9.7%)	0.0950 (19.2%)	0.1062 (15.6%)
	✓			0.0984 (5.8%)	0.1451 (5.5%)	0.0830 (5.7%)	0.0976 (5.4%)	0.1025 (11.3%)	0.1447 (11.0%)	0.0881 (10.5%)	0.1015 (10.4%)
		✓		0.1052 (13.1%)	0.1528 (11.1%)	0.0891 (13.5%)	0.1039 (12.2%)	0.1230 (33.6%)	0.1671 (28.1%)	0.1092 (37.0%)	0.1226 (33.4%)
✓	✓			0.1071 (15.2%)	0.1569 (14.1%)	0.0908 (15.7%)	0.1064 (14.9%)	0.1253 (36.0%)	0.1704 (30.7%)	0.1111 (39.4%)	0.1248 (35.8%)
✓	✓	✓		0.1067 (14.7%)	0.1555 (13.1%)	0.0904 (15.2%)	0.1057 (14.1%)	0.1261 (36.9%)	0.1701 (30.4%)	0.1118 (40.3%)	0.1251 (36.1%)
✓	✓	✓	✓	0.1196 (28.6%)	0.1743 (26.8%)	0.1010 (28.7%)	0.1182 (27.6%)	0.1320 (43.3%)	0.1797 (37.8%)	0.1160 (45.5%)	0.1305 (42.0%)

Component				Gowalla				Yelp2022			
HS	PI	HA	GP	Recall@10	Recall@20	NDCG@10	NDCG@20	Recall@10	Recall@20	NDCG@10	NDCG@20
				0.1224 (0.0%)	0.1815 (0.0%)	0.1172 (0.0%)	0.1348 (0.0%)	0.0641 (0.0%)	0.1082 (0.0%)	0.0536 (0.0%)	0.0678 (0.0%)
✓				0.1266 (3.4%)	0.1843 (1.5%)	0.1228 (4.8%)	0.1393 (3.3%)	0.0697 (8.7%)	0.1148 (6.1%)	0.0584 (9.0%)	0.0728 (7.4%)
	✓			0.1330 (8.7%)	0.1974 (8.8%)	0.1284 (9.6%)	0.1475 (9.4%)	0.0715 (11.5%)	0.1179 (9.0%)	0.0597 (11.4%)	0.0746 (10.0%)
		✓		0.1376 (12.4%)	0.1981 (9.1%)	0.1338 (14.2%)	0.1512 (12.2%)	0.0769 (20.0%)	0.1242 (14.8%)	0.0644 (20.1%)	0.0795 (17.3%)
✓	✓			0.1411 (15.3%)	0.2083 (14.8%)	0.1354 (15.5%)	0.1550 (15.0%)	0.0775 (20.9%)	0.1247 (15.2%)	0.0650 (21.3%)	0.0800 (18.0%)
✓	✓	✓		0.1447 (18.2%)	0.2086 (14.9%)	0.1396 (19.1%)	0.1581 (17.3%)	0.0790 (23.2%)	0.1273 (17.7%)	0.0660 (23.1%)	0.0814 (20.1%)
✓	✓	✓	✓	0.1576 (28.8%)	0.2273 (25.2%)	0.1532 (30.7%)	0.1734 (28.6%)	0.0795 (24.0%)	0.1280 (18.3%)	0.0670 (25.0%)	0.0824 (21.5%)

improvement peaks at 39.4%. This highlights the importance of initialization for hyperbolic models, as our PI can provide more informative prior knowledge for the initial embedding.

- Incorporating HA with HS likewise yields performance enhancements across all datasets (row 4 in Table 2). However, when combined with PI, the performance (row 6 in Table 2) varies among datasets compared to row 5 in Table 2: remaining unchanged for Amazon-CD and Amazon-Book, while seeing a boost for Gowalla and Yelp2022 datasets. This seems to correlate with dataset types, namely purchase and check-in datasets respectively, suggesting that the efficacy of HA may be dataset-type dependent. In our experiments, HA’s impact is more evident in the check-in datasets.
- HS and PI+HA are complementary, as their combination produces an improvement equivalent to  $1+2>3$  in metrics (refer to rows 2, 3, and 6 in Table 2). This can be attributed to their distinct model enhancement aspects, namely model training, model initialization, and model structure respectively.
- Upon introducing GP (HGCH+) (row 7 in Table 2), the model performance is further enhanced, particularly for Amazon-CD, which sees the highest further improvement rate of 13.9% compared to HGCH (row 6 in Table 2). This verifies the effectiveness of GP and side information. However, the improvement for Yelp2022 is less pronounced, possibly due to the limited utility and noises of its side information in the recommendation task.

## 6.5 Comparison of Fusion Methods (RQ3)

We conducted an empirical evaluation to assess the impact of different fusion methods on the model performance. Fig. 4 illustrates the results of the fusion methods that we introduced in Section 4.2.2, where the Base is the version without side information, and B, G, P, and GP denote Base, Gate, Prior, and Gate&Prior, respectively. We observe two salient phenomena:

- Except for gate in the Yelp2022 dataset, all three fusion methods bring performance improvement compared to the Base, indicating

that these fusion methods basically incorporate side information into embedding.

- The Gate and Prior methods’ efficacy depends on specific factors. Gate excels in large datasets, outperforming other methods on the Amazon-Book dataset. Conversely, Prior maintains good performance in most cases. However, both struggle with high noise levels in side information, demonstrated by their decreased performance in Yelp2022’s noisy data.<sup>5</sup> Under such conditions, their efficiency falls below Base. The combined Gate&Prior method shows stable improvement across datasets, highlighting its capability to adjust weights effectively based on Prior.

## 6.6 Embedding Visualization Analysis (RQ4)

In this section, we aim to provide a plausible interpretation of our proposed approach by visualizing the embedding learned by HGCH. Since our model employs the Poincaré disc as its underlying geometry, it facilitates the visualization process. We adopt a 3-layer HGCH model with an embedding size of 2 for visualization purposes, following the previous work [9, 33]. To comprehend the learned embeddings, we select the Amazon-Book dataset as an exemplar, assign the quartiles of the number of interactions as node labels with different colors, and display the embeddings before and after graph convolution.

As showed in Fig. 5, before graph convolution, with uniform initialization, item embeddings show a Gaussian-like spread. After applying power law prior-based initialization and then adding side information, popular items cluster near the origin, indicating enhanced embedding training. After graph convolution, embeddings with power law prior-based initialization exhibit clearer class boundaries compared to uniform initialization. Moreover, integrating side information further congregates popular nodes near the origin, suggesting its effectiveness in performance improvement by aligning node distribution with popularity.

<sup>5</sup>Yelp2022’s noise in side information also significantly impacts HGCF, HRCF, and HICF, as shown in Table 1.

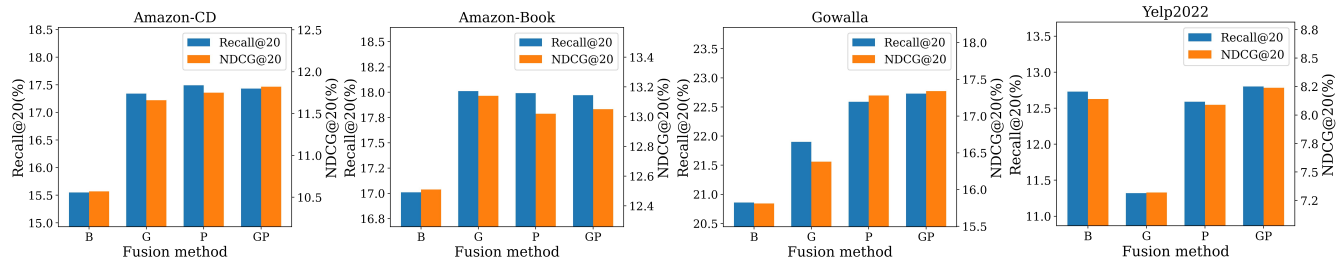


Figure 4: Comparison between different fusion methods. B, G, P, and GP represent Base, Gate, Prior, and Gate&Prior, respectively, where the Base is the HGCH.

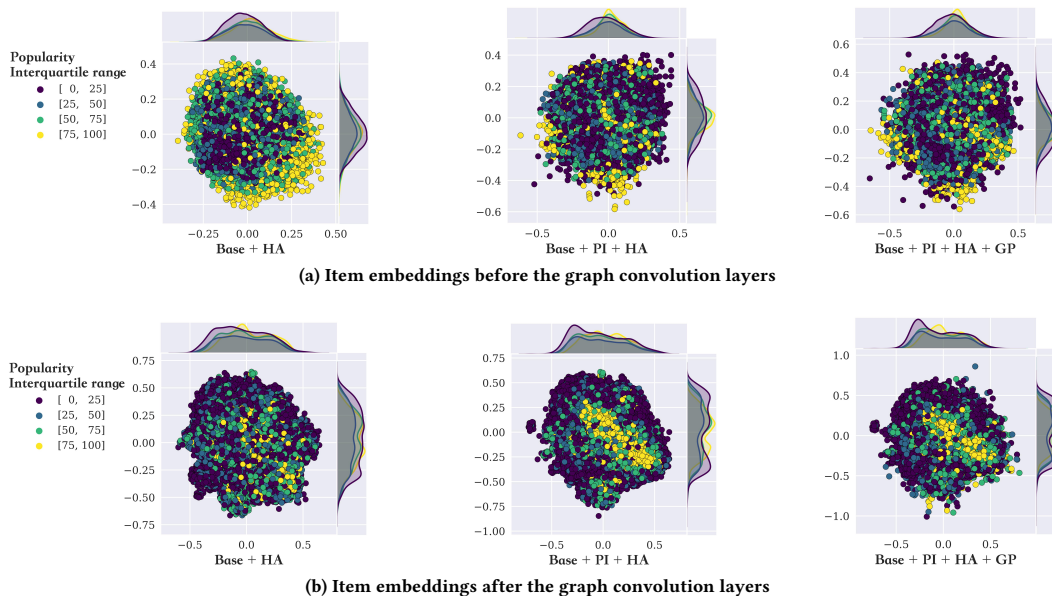


Figure 5: HGCH item embedding visualization in the Poincaré representation of tangent space before and after the graph convolutional layers on the dataset Amazon-Book. Items are categorized into quartiles by popularity, where [75, 100] represents the most popular items. The meaning of Base, PI, HA, and GP are the same as in Section 6.4.

## 6.7 Convergent Speed (RQ5)

We also examine the convergence behavior of our proposed HGCH model compared to other hyperbolic models throughout the training process. Fig. 1 shows the NDCG@10 metrics on the validation set from 1 to 1000 epochs. Similar patterns are observed for other metrics@Ks. Notably, HGCH demonstrates exceptionally rapid convergence, allowing us to limit its training to 40 epochs on Amazon-Book and 60 epochs on Yelp2022, thereby saving computational resources. Additionally, on Yelp, HGCF shows no improvement in NDCG@10 during the last 100 epochs of training, leading to early termination. From these observations, we can draw the following conclusions: (1) our HGCH consistently outperforms all baseline models across all epochs, showing significant improvement; and (2) our approach achieves peak performance in fewer epochs, indicating that our hyperbolic sampling method accelerates the training process effectively.

## 7 Conclusion

In this paper, we propose HGCH, a HGCN-based collaborative filtering model that improves the HGCN structure and incorporates multiple kinds of side information into a heterogeneous collaborative graph, as well as greatly speeds up the training convergence speed. Experiments conducted on four real-world datasets showed significant improvements compared to the baseline and better utilization of hyperbolic space (as evidenced by better utilization of exponentially increased capacity to pay more attention to tail items), which is beneficial for personalized recommendations and increasing market diversity [48]. We believe it will bring new insights into HGCN-based recommender systems.

## References

- [1] Aaron B. Adcock, Blair D. Sullivan, and Michael W. Mahoney. 2013. Tree-Like Structure in Large Social and Information Networks. In *2013 IEEE 13th International Conference on Data Mining*. 1–10.

- [2] Dzmitry Bahdanau, Kyunghyun Cho, and Yoshua Bengio. 2015. Neural Machine Translation by Jointly Learning to Align and Translate. In *3rd International Conference on Learning Representations, ICLR 2015, San Diego, CA, USA, May 7-9, 2015, Conference Track Proceedings*, Yoshua Bengio and Yann LeCun (Eds.). <http://arxiv.org/abs/1409.0473>
- [3] Jasmijn Bastings, Ivan Titov, Wilker Aziz, Diego Marcheggiani, and Khalil Sima'an. 2017. Graph Convolutional Encoders for Syntax-aware Neural Machine Translation. In *Proceedings of the 2017 Conference on Empirical Methods in Natural Language Processing*. Association for Computational Linguistics, Copenhagen, Denmark, 1957–1967.
- [4] Ines Chami, Zhitao Ying, Christopher Ré, and Jure Leskovec. 2019. Hyperbolic Graph Convolutional Neural Networks. In *Advances in Neural Information Processing Systems*, H. Wallach, H. Larochelle, A. Beygelzimer, F. d'Alché-Buc, E. Fox, and R. Garnett (Eds.), Vol. 32. Curran Associates, Inc.
- [5] Weize Chen, Xu Han, Yankai Lin, Hexu Zhao, Zhiyuan Liu, Peng Li, Maosong Sun, and Jie Zhou. 2022. Fully Hyperbolic Neural Networks. In *Proceedings of the 60th Annual Meeting of the Association for Computational Linguistics (Volume 1: Long Papers)*. Association for Computational Linguistics, Dublin, Ireland, 5672–5686. <https://doi.org/10.18653/v1/2022.acl-long-389>
- [6] Yankai Chen, Menglin Yang, Yingxue Zhang, Mengchen Zhao, Ziqiao Meng, Jianye Hao, and Irwin King. 2022. Modeling Scale-Free Graphs with Hyperbolic Geometry for Knowledge-Aware Recommendation. In *Proceedings of the Fifteenth ACM International Conference on Web Search and Data Mining (Virtual Event, AZ, USA) (WSDM '22)*. Association for Computing Machinery, New York, NY, USA, 94–102.
- [7] Eunjoon Cho, Seth A Myers, and Jure Leskovec. 2011. Friendship and mobility: user movement in location-based social networks. In *Proceedings of the 17th ACM SIGKDD international conference on Knowledge discovery and data mining*. 1082–1090.
- [8] David K Duvenaud, Dougal Maclaurin, Jorge Iparraguirre, Rafael Bombarell, Timothy Hirzel, Alán Aspuru-Guzik, and Ryan P Adams. 2015. Convolutional networks on graphs for learning molecular fingerprints. *Advances in neural information processing systems* 28 (2015).
- [9] Shanshan Feng, Lucas Vinh Tran, Gao Cong, Lisi Chen, Jing Li, and Fan Li. 2020. Hme: A hyperbolic metric embedding approach for next-poi recommendation. In *Proceedings of the 43rd International ACM SIGIR Conference on Research and Development in Information Retrieval*. 1429–1438.
- [10] Alex Fout, Jonathon Byrd, Basir Shariat, and Asa Ben-Hur. 2017. Protein interface prediction using graph convolutional networks. *Advances in neural information processing systems* 30 (2017).
- [11] Xavier Glorot and Yoshua Bengio. 2010. Understanding the difficulty of training deep feedforward neural networks. In *Proceedings of the Thirteenth International Conference on Artificial Intelligence and Statistics (Proceedings of Machine Learning Research, Vol. 9)*, Yee Whye Teh and Mike Titterton (Eds.). PMLR, Chia Laguna Resort, Sardinia, Italy, 249–256.
- [12] Ruining He and Julian McAuley. 2016. Ups and downs: Modeling the visual evolution of fashion trends with one-class collaborative filtering. In *proceedings of the 25th international conference on world wide web*. 507–517.
- [13] Xiangnan He, Kuan Deng, Xiang Wang, Yan Li, YongDong Zhang, and Meng Wang. 2020. LightGCN: Simplifying and Powering Graph Convolution Network for Recommendation. In *Proceedings of the 43rd International ACM SIGIR Conference on Research and Development in Information Retrieval (Virtual Event, China) (SIGIR '20)*. Association for Computing Machinery, New York, NY, USA, 639–648.
- [14] Binbin Hu, Chuan Shi, Wayne Xin Zhao, and Philip S Yu. 2018. Leveraging meta-path based context for top-n recommendation with a neural co-attention model. In *Proceedings of the 24th ACM SIGKDD international conference on knowledge discovery & data mining*. 1531–1540.
- [15] Binbin Hu, Chuan Shi, Wayne Xin Zhao, and Philip S Yu. 2018. Leveraging meta-path based context for top-n recommendation with a neural co-attention model. In *Proceedings of the 24th ACM SIGKDD international conference on knowledge discovery & data mining*. 1531–1540.
- [16] Yifan Hu, Yehuda Koren, and Chris Volinsky. 2008. Collaborative Filtering for Implicit Feedback Datasets. In *2008 Eighth IEEE International Conference on Data Mining*. IEEE, Pisa, Italy, 263–272.
- [17] Kalervo Järvelin and Jaana Kekäläinen. 2002. Cumulated gain-based evaluation of IR techniques. *ACM Transactions on Information Systems (TOIS)* 20, 4 (2002), 422–446.
- [18] Jiarui Jin, Jiarui Qin, Yuchen Fang, Kouninghua Du, Weinan Zhang, Yong Yu, Zheng Zhang, and Alexander J Smola. 2020. An efficient neighborhood-based interaction model for recommendation on heterogeneous graph. In *Proceedings of the 26th ACM SIGKDD international conference on knowledge discovery & data mining*. 75–84.
- [19] Steven Kearnes, Kevin McCloskey, Marc Berndl, Vijay Pande, and Patrick Riley. 2016. Molecular graph convolutions: moving beyond fingerprints. *Journal of computer-aided molecular design* 30, 8 (2016), 595–608.
- [20] Diederick P Kingma and Jimmy Ba. 2015. Adam: A method for stochastic optimization. In *International Conference on Learning Representations (ICLR)*.
- [21] Zekun Li, Yujia Zheng, Shu Wu, Xiaoyu Zhang, and Liang Wang. 2020. Heterogeneous graph collaborative filtering. *arXiv preprint arXiv:2011.06807* (2020).
- [22] Chundi Liu, Guangwei Yu, Maksims Volkovs, Cheng Chang, Himanshu Rai, Junwei Ma, and Satya Krishna Gorti. 2019. Guided Similarity Separation for Image Retrieval. In *Advances in Neural Information Processing Systems*, H. Wallach, H. Larochelle, A. Beygelzimer, F. d'Alché-Buc, E. Fox, and R. Garnett (Eds.), Vol. 32. Curran Associates, Inc.
- [23] Qi Liu, Maximilian Nickel, and Douwe Kiela. 2019. Hyperbolic Graph Neural Networks. In *Advances in Neural Information Processing Systems*, H. Wallach, H. Larochelle, A. Beygelzimer, F. d'Alché-Buc, E. Fox, and R. Garnett (Eds.), Vol. 32. Curran Associates, Inc.
- [24] Kelong Mao, Jieming Zhu, Xi Xiao, Biao Lu, Zhaowei Wang, and Xiuqiang He. 2021. UltraGCN: Ultra Simplification of Graph Convolutional Networks for Recommendation. In *Proceedings of the 30th ACM International Conference on Information & Knowledge Management (Virtual Event, Queensland, Australia) (CIKM '21)*. Association for Computing Machinery, New York, NY, USA, 1253–1262. <https://doi.org/10.1145/3459637.3482291>
- [25] D Marcheggiani and I Titov. 2017. Encoding sentences with graph convolutional networks for semantic role labeling. In *EMNLP 2017-Conference on Empirical Methods in Natural Language Processing, Proceedings*. 1506–1515.
- [26] Leyla Mirvakhabova, Evgeny Frolov, Valentin Khruikov, Ivan Oseledets, and Alexander Tuzhilin. 2020. Performance of Hyperbolic Geometry Models on Top-N Recommendation Tasks. In *Proceedings of the 14th ACM Conference on Recommender Systems (Virtual Event, Brazil) (RecSys '20)*. Association for Computing Machinery, New York, NY, USA, 527–532.
- [27] Maximilian Nickel and Douwe Kiela. 2017. Poincaré embeddings for learning hierarchical representations. *Advances in neural information processing systems* 30 (2017).
- [28] Mathias Niepert, Mohamed Ahmed, and Konstantin Kutzkov. 2016. Learning Convolutional Neural Networks for Graphs. In *Proceedings of The 33rd International Conference on Machine Learning (Proceedings of Machine Learning Research, Vol. 48)*, Maria Florina Balcan and Kilian Q. Weinberger (Eds.). PMLR, New York, New York, USA, 2014–2023.
- [29] Shaowen Peng, Kazunari Sugiyama, and Tsunenori Mine. 2022. SVD-GCN: A Simplified Graph Convolution Paradigm for Recommendation (CIKM '22). Association for Computing Machinery, New York, NY, USA, 1625–1634. <https://doi.org/10.1145/3511808.3557462>
- [30] Erzsébet Ravasz and Albert-László Barabási. 2003. Hierarchical organization in complex networks. *Physical review E* 67, 2 (2003), 026112.
- [31] Steffen Rendle, Christoph Freudenthaler, Zeno Gantner, and Lars Schmidt-Thieme. 2009. BPR: Bayesian Personalized Ranking from Implicit Feedback. In *Proceedings of the Twenty-Fifth Conference on Uncertainty in Artificial Intelligence (UAI '09)*. AUAI Press, Arlington, Virginia, USA, 452–461.
- [32] Jinghan Shi, Houye Ji, Chuan Shi, Xiao Wang, Zhiqiang Zhang, and Jun Zhou. 2020. Heterogeneous graph neural network for recommendation. *arXiv preprint arXiv:2009.00799* (2020).
- [33] Jianjun Sun, Zhaoyue Cheng, Saba Zuberi, Felipe Perez, and Maksims Volkovs. 2021. HGCF: Hyperbolic Graph Convolution Networks for Collaborative Filtering. In *Proceedings of the Web Conference 2021 (WWW '21)*. Association for Computing Machinery, New York, NY, USA, 593–601.
- [34] Yizhou Sun, Jiawei Han, Xifeng Yan, Philip S Yu, and Tianyi Wu. 2011. Pathsim: Meta path-based top-k similarity search in heterogeneous information networks. *Proceedings of the VLDB Endowment* 4, 11 (2011), 992–1003.
- [35] Zhu Sun, Jie Yang, Jie Zhang, Alessandro Bozzon, Long-Kai Huang, and Chi Xu. 2018. Recurrent knowledge graph embedding for effective recommendation. In *Proceedings of the 12th ACM conference on recommender systems*. 297–305.
- [36] Abraham Albert Ungar. 2008. A gyrovector space approach to hyperbolic geometry. *Synthesis Lectures on Mathematics and Statistics* 1, 1 (2008), 1–194.
- [37] Lucas Vinh Tran, Yi Tay, Shuai Zhang, Gao Cong, and Xiaoli Li. 2020. HyperML: A Boosting Metric Learning Approach in Hyperbolic Space for Recommender Systems (WSDM '20). Association for Computing Machinery, New York, NY, USA, 609–617.
- [38] Hao Wang, Defu Lian, Hanghang Tong, Qi Liu, Zhenya Huang, and Enhong Chen. 2021. HyperSoRec: Exploiting Hyperbolic User and Item Representations with Multiple Aspects for Social-Aware Recommendation. 40, 2, Article 24 (sep 2021), 28 pages.
- [39] Liping Wang, Fenyu Hu, Shu Wu, and Liang Wang. 2021. Fully Hyperbolic Graph Convolution Network for Recommendation. In *Proceedings of the 30th ACM International Conference on Information & Knowledge Management (Virtual Event, Queensland, Australia) (CIKM '21)*. Association for Computing Machinery, New York, NY, USA, 3483–3487.
- [40] Xiang Wang, Xiangnan He, Yixin Cao, Meng Liu, and Tat-Seng Chua. 2019. Kgat: Knowledge graph attention network for recommendation. In *Proceedings of the 25th ACM SIGKDD international conference on knowledge discovery & data mining*. 950–958.
- [41] Xiang Wang, Xiangnan He, Meng Wang, Fuli Feng, and Tat-Seng Chua. 2019. Neural Graph Collaborative Filtering. In *Proceedings of the 42nd International ACM SIGIR Conference on Research and Development in Information Retrieval (Paris, France) (SIGIR '19)*. Association for Computing Machinery, New York, NY,

- USA, 165–174.
- [42] Xiang Wang, Hongye Jin, An Zhang, Xiangnan He, Tong Xu, and Tat-Seng Chua. 2020. Disentangled Graph Collaborative Filtering. In *Proceedings of the 43rd International ACM SIGIR Conference on Research and Development in Information Retrieval* (Virtual Event, China) (SIGIR '20). Association for Computing Machinery, New York, NY, USA, 1001–1010.
- [43] Xiang Wang, Dingxian Wang, Canran Xu, Xiangnan He, Yixin Cao, and Tat-Seng Chua. 2019. Explainable reasoning over knowledge graphs for recommendation. In *Proceedings of the AAAI conference on artificial intelligence*, Vol. 33. 5329–5336.
- [44] Max Welling and Thomas N Kipf. 2016. Semi-supervised classification with graph convolutional networks. In *J. International Conference on Learning Representations (ICLR 2017)*.
- [45] Danfei Xu, Yuke Zhu, Christopher B. Choy, and Li Fei-Fei. 2017. Scene Graph Generation by Iterative Message Passing. In *Proceedings of the IEEE Conference on Computer Vision and Pattern Recognition (CVPR)*.
- [46] Zhirong Xu, Shiyang Wen, Junshan Wang, Guojun Liu, Liang Wang, Zhi Yang, Lei Ding, Yan Zhang, Di Zhang, Jian Xu, and Bo Zheng. 2022. AMCAD: Adaptive Mixed-Curvature Representation based Advertisement Retrieval System. In *2022 IEEE 38th International Conference on Data Engineering (ICDE)*. 3439–3452. <https://doi.org/10.1109/ICDE53745.2022.00323>
- [47] Jianwei Yang, Jiasen Lu, Stefan Lee, Dhruv Batra, and Devi Parikh. 2018. Graph R-CNN for Scene Graph Generation. In *Proceedings of the European Conference on Computer Vision (ECCV)*.
- [48] Menglin Yang, Zhihao Li, Min Zhou, Jiahong Liu, and Irwin King. 2022. HICF: Hyperbolic Informative Collaborative Filtering. In *Proceedings of the 28th ACM SIGKDD Conference on Knowledge Discovery and Data Mining* (Washington DC, USA) (KDD '22). Association for Computing Machinery, New York, NY, USA, 2212–2221.
- [49] Menglin Yang, Min Zhou, Jiahong Liu, Defu Lian, and Irwin King. 2022. HRCF: Enhancing Collaborative Filtering via Hyperbolic Geometric Regularization. In *Proceedings of the ACM Web Conference 2022* (Virtual Event, Lyon, France) (WWW '22). Association for Computing Machinery, New York, NY, USA, 2462–2471.
- [50] Xiao Yu, Xiang Ren, Quanquan Gu, Yizhou Sun, and Jiawei Han. 2013. Collaborative filtering with entity similarity regularization in heterogeneous information networks. *IJCAI HINA 27* (2013).
- [51] Sixiao Zhang, Hongxu Chen, Xiao Ming, Lizhen Cui, Hongzhi Yin, and Guandong Xu. 2021. Where Are We in Embedding Spaces?. In *Proceedings of the 27th ACM SIGKDD Conference on Knowledge Discovery & Data Mining* (Virtual Event, Singapore) (KDD '21). Association for Computing Machinery, New York, NY, USA, 2223–2231.
- [52] Yiding Zhang, Xiao Wang, Chuan Shi, Nian Liu, and Guojie Song. 2021. Lorentzian Graph Convolutional Networks. In *Proceedings of the Web Conference 2021* (Ljubljana, Slovenia) (WWW '21). Association for Computing Machinery, New York, NY, USA, 1249–1261.
- [53] Wayne Xin Zhao, Shanlei Mu, Yupeng Hou, Zihan Lin, Yushuo Chen, Xingyu Pan, Kaiyuan Li, Yujie Lu, Hui Wang, Changxin Tian, et al. 2021. Rebole: Towards a unified, comprehensive and efficient framework for recommendation algorithms. In *Proceedings of the 30th ACM International Conference on Information & Knowledge Management*.

**Table 3: Interaction information statistics for datasets.**

Dataset	#User	#Item	#Interaction	Density
Amazon-CD	16865	33900	476676	0.083%
Amazon-Book	109730	96421	3181759	0.030%
Gowalla	29858	40988	1027464	0.084%
Yelp2022	93537	53347	2533759	0.051%

**Table 4: Side information statistics for datasets. U, I, and C represent user, item, and category respectively.**

Dataset	Relation (A-B)	#A	#B	#A-B
Amazon-CD	category (C-I)	380	33900	68382
	also_buy (I-I)	33900	33900	121149
	also_view (I-I)	33900	33900	121149
Amazon-Book	category (C-I)	457	96421	171257
	also_buy (I-I)	96421	96421	347311
	also_view (I-I)	96421	96421	159154
Gowalla	friend (U-U)	29858	29858	279478
	neighbor (I-I)	40988	40988	501242
Yelp2022	friend (U-U)	93537	93537	1295854
	neighbor (I-I)	53347	53347	1038744

## A Analysis of Gyromidpoint

Here, we try to analyze more specifically how the neighbor aggregation through gyromidpoint differs from the way by tangent space, to explain why hyperbolic neighbor aggregation may be more effective. Substituting Eq. (10) into  $\lambda(k, \mathbf{h}_i)$  and omit the notation of subspace and the number of layer for simplicity, we get:

$$\begin{aligned}
\lambda(k, \mathbf{h}_i) &= 2 \left( 1 - \frac{\|\mathbf{h}_i\|^2}{k} \right)^{-1} \\
&= 2 \left( 1 - \frac{\|\exp_0^k(\mathbf{e}_i)\|^2}{k} \right)^{-1} \\
&= 2 \left( 1 - \frac{\|\tanh\left(\frac{\|\mathbf{e}_i\|}{\sqrt{k}}\right) \frac{\sqrt{k}\mathbf{e}_i}{\|\mathbf{e}_i\|}\|^2}{k} \right)^{-1} \\
&= 2 \left( 1 - \tanh^2\left(\frac{\|\mathbf{e}_i\|}{\sqrt{k}}\right) \right)^{-1}.
\end{aligned}$$

We notice that when fixing the negative reciprocal of the curvature  $k$ , the magnitude of  $\lambda(k, \mathbf{h}_i)$  positively correlates with the magnitude of  $\mathbf{e}_i$ . Furthermore, the role of  $\lambda(k, \mathbf{h}_i)$  in Eq. (9) is similar to the weight of node  $\mathbf{h}_i$ , which means that the node with a larger embedding magnitude in tangent space has a more significant weight in neighbor aggregation. Therefore, combining the relationship between embedding magnitude and popularity in hyperbolic space, we can find that: in gyromidpoint neighbor aggregation, nodes with lower popularity are more likely to contribute more. While tangent space neighbor aggregation only directly averages all the nodes being aggregated, and its corresponding Laplace matrix is  $\mathbf{D}^{-1}\mathbf{A}$  ( $\mathbf{A}$  is the adjacency matrix, and  $\mathbf{D}$  is the degree matrix), which does not explicitly weaken the contribution of high popularity nodes,

thus may lead to the degradation of performance. There is also a commonly used Laplacian matrix of  $\mathbf{D}^{-\frac{1}{2}}\mathbf{A}\mathbf{D}^{-\frac{1}{2}}$ , which does a second averaging according to the popularity of the nodes being aggregated, but in practice, it yields a worse performance under the hyperbolic space scenario.

## B DATASETS AND BASELINES

### B.1 Dataset Description

In this section, we give the detailed descriptions and pre-processing of the four datasets.

**Amazon-CD** and **Amazon-Book**: Amazon-review is a widely used dataset for product recommendations [12]. Following previous work [33], we select Amazon-CD and Amazon-Book from this set and transform the ratings into binary preferences with a threshold  $\geq 4$  to simulate implicit feedback. To ensure the data quality, we use a 10-core setting and a 5-core setting for Amazon-CD for users and items, respectively, *i.e.*, retaining users with at least ten interactions and items with five interactions. Moreover, a 10-core setting is used for Amazon-Book.

**Gowalla**: This is a dataset collected from gowalla, a location-based social networking website where users share their locations by checking in [7]. Here, we consider the location as the item. We also use a 10-core to ensure data quality.

**Yelp2022**: This dataset is adopted from the 2022 edition of the yelp website. Here, we consider local businesses like restaurants and bars as the item. Again, we use a 10-core setting to ensure that the user and item have at least ten interactions.

Moreover, we need to build side information bipartite graphs (referred to as side graphs for short) for each dataset. For Amazon-CD and Amazon-Book, we choose {category (C-C), also\_buy (I-I), also\_view (I-I)}. For Gowalla and Yelp2022, we first choose social information (U-U) and then construct geographic neighborhood information (I-I) from latitude and longitude, which is an important feature in poi recommendation. We approximate the earth as a sphere with a radius of 6371 km and use the haversine<sup>6</sup> function to calculate the geographical distance  $d_{geo}$  between two locations. Locations within a geographical distance of 0.2 km are considered neighbors and form the geographical neighbor graph.

We present the statistics of historical interaction data and side information for the four datasets in Table 3 and Table 4. For each dataset, we divide it into a training set and a test set with the ratio of 8:2. Then, for tuning hyperparameters, 10% of the training set is randomly selected as the validation set.

### B.2 Baselines and Settings

This section gives clear descriptions and settings of the baselines used in our experiments.

To show the effectiveness of our model, we compare our proposed HGCH with latent factor-based (BPRMF [31] and WRMF [16]), graph neural network-based (NGCF [41], LightGCN [13], and DGCF [42]), and hyperbolic neural network-based (HGCF [33], HRCF [49], and HICF [48]):

- **BPRMF** [31] is based on Bayesian personalized ranking, which models the order of candidate items by pairwise ranking loss.

<sup>6</sup>[https://en.wikipedia.org/wiki/Haversine\\_formula](https://en.wikipedia.org/wiki/Haversine_formula).

**Table 5: Performance of HGCH with different subsets of components on the H20 and T80 items for dataset Amazon-Book and Yelp2022.**

Component					Amazon-Book							
					Recall@20		Recall@10		NDCG@20		NDCG@10	
HS	PI	HA	GP		H20	T80	H20	T80	H20	T80	H20	T80
					0.1143(0.0%)	0.0445(0.0%)	0.0813(0.0%)	0.0315(0.0%)	0.0819(0.0%)	0.0325(0.0%)	0.0717(0.0%)	0.0285(0.0%)
✓					0.1232(7.8%)	0.0490(10.1%)	0.0922(13.4%)	0.0368(16.8%)	0.0937(14.4%)	0.0376(15.7%)	0.0847(18.1%)	0.0340(19.3%)
	✓	✓			0.1247(9.1%)	0.0512(15.1%)	0.0889(9.3%)	0.0368(16.8%)	0.0894(9.2%)	0.0378(16.3%)	0.0784(9.3%)	0.0333(16.8%)
			✓		0.1399(22.4%)	0.0600(34.8%)	0.1049(29.0%)	0.0450(42.9%)	0.1059(29.3%)	0.0458(40.9%)	0.0957(33.5%)	0.0414(45.3%)
✓	✓				0.1423(24.5%)	0.0616(38.4%)	0.1063(30.8%)	0.0463(47.0%)	0.1076(31.4%)	0.0469(44.3%)	0.0972(35.6%)	0.0424(48.8%)
✓	✓	✓			0.1418(24.1%)	0.0610(37.1%)	0.1070(31.6%)	0.0459(45.7%)	0.1078(31.6%)	0.0470(44.6%)	0.0978(36.4%)	0.0426(49.5%)
✓	✓	✓	✓		0.1458(27.6%)	0.0698(56.9%)	0.1093(34.4%)	0.0524(66.3%)	0.1102(34.6%)	0.0529(62.8%)	0.0997(39.1%)	0.0479(68.1%)

Component					Yelp2022							
					Recall@20		Recall@10		NDCG@20		NDCG@10	
HS	PI	HA	GP		H20	T80	H20	T80	H20	T80	H20	T80
					0.1087(0.0%)	0.0365(0.0%)	0.0660(0.0%)	0.0217(0.0%)	0.0688(0.0%)	0.0234(0.0%)	0.0551(0.0%)	0.0186(0.0%)
✓					0.1156(6.3%)	0.0377(3.3%)	0.0718(8.8%)	0.0231(6.5%)	0.0741(7.7%)	0.0247(5.6%)	0.0603(9.4%)	0.0201(8.1%)
	✓	✓			0.1166(7.3%)	0.0384(5.2%)	0.0719(8.9%)	0.0232(6.9%)	0.0742(7.8%)	0.0249(6.4%)	0.0600(8.9%)	0.0201(8.1%)
			✓		0.1236(13.7%)	0.0411(12.6%)	0.0782(18.5%)	0.0253(16.6%)	0.0800(16.3%)	0.0270(15.4%)	0.0656(19.1%)	0.0220(18.3%)
✓	✓				0.1239(14.0%)	0.0429(17.5%)	0.0783(18.6%)	0.0266(22.6%)	0.0803(16.7%)	0.0281(20.1%)	0.0659(19.6%)	0.0229(23.1%)
✓	✓	✓			0.1257(15.6%)	0.0439(20.3%)	0.0797(20.8%)	0.0271(24.9%)	0.0814(18.3%)	0.0286(22.2%)	0.0668(21.2%)	0.0233(25.3%)
✓	✓	✓	✓		0.1266(16.5%)	0.0453(24.1%)	0.0803(21.7%)	0.0280(29.0%)	0.0824(19.8%)	0.0297(26.9%)	0.0678(23.0%)	0.0243(30.6%)

- **WRMF** [16] is a classical latent factor model that attaches a weight to each training sample to characterize the confidence level of the user’s preference for the items.
- **NGCF** [41] is a GCN-based model that explores high-order connectivity in the user-item graph by propagating embedding and injects collaboration signals into the embedding explicitly.
- **LightGCN** [13] is a state-of-the-art GCN model, which removes feature transformations and nonlinear activations that are useless for collaborative filtering in GCN.
- **DGCF** [42] uses GCN to encode graph structure data and iteratively refines intention-aware interaction graphs and representations by modeling the intention distribution of each user-item interaction. Here, we follow the original paper to set its graph disentangling layer to 1 because of high computational cost.
- **HGCF** [33] is a leading hyperbolic GCN model, which replaces the traditional Euclidean space with Lorentz space, and learns embedding by Skip-GCN structure and margin ranking loss.
- **HRCF** [49] is a leading hyperbolic GCN model, which is based on HGCF and adds a geometry-aware hyperbolic regularizer to boost optimization.
- **HICF** [48] is a state-of-the-art hyperbolic GCN model, which is also based on HGCF and adapt the hyperbolic margin ranking learning, making its pull and push procedure geometric-aware, then providing informative guidance for the learning of both head and tail items.

Besides, we refer to the version using HCG directly as HGCF+, HRCF+, and HICF+, respectively. For our model, we denote the version that uses only the user-item bipartite graph and the version that utilizes HCG as HGCH and HGCH+, respectively. Note that the main difference between HGCF+/HRCF+/HICF+ and HGCH+ is the neighbor aggregation, the former proceeds directly on the HCG, but the latter performs on each subgraph of the HCG separately.

We used RecBole [53] to implement our models and baselines. We followed the original settings and tuned the parameters for each

model. The embedding size was 64 for all models. We used Adam optimizer [20] for most models except HGCFs/HRCFs/HICFs which used RSGD. The gate parameters of HGCH+ and the parameters of other models are initialized using Xavier initializer [11] except for the embedding weight of HGCFs/HRCFs/HICFs and HGCHs, which use uniform initializer and power law prior-based initializer, respectively. For NGCF, LightGCN, HGCFs, and HGCHs, we set their GCN layers to 3.<sup>7</sup> We apply a grid search to the hyperparameters: the batch size of the different models on each dataset is tuned in {1024, 2048, 4096, 8192} and the learning rate is tuned amongst {0.01, 0.005, 0.001, 0.0005, 0.0001}, weight decay or  $L_2$  normalization is search in {0.01, 0.005,  $\dots$ ,  $5 \times 10^{-5}, 10^{-6}$ }, and the dropout ratio is tuned in {0.0, 0.1,  $\dots$ , 0.5} for NCF, NGCF. Besides, we employ the node dropout technique for NGCF, where the ratio is searched in {0.0, 0.1,  $\dots$ , 0.5}. For WRMF, we select the positive item weight from {1, 10, 100, 1000, 10000}. For NCF, the ratio of positive and negative samples for negative sampling is 1:4, which follows the original setting. For DGCF, the iteration number and latent intents are set to 2 and 4, respectively, and the correlation weight is tuned amongst {0.005, 0.01, 0.02, 0.05}. For HRCF, the  $\lambda$  in the loss function is in the range of {10, 15, 20, 25, 30} and the layers of GCN is searched from 2 to 10.<sup>8</sup> For HICF, the margin is selected from {0.4, 0.5,  $\dots$ , 1.0}, the  $n_{neg}$  is tuned in {5, 10, 20,  $\dots$ , 100}, and the layers of GCN is searched from 2 to 6. For our model, we set all curvatures to 1 for simplicity, leaving the exploration of different hyperbolic subspace curvatures with possible performance gains to future work. The hyperparameter of power law distribution  $b$  and auxiliary task weight  $\alpha$  are empirically set to 1.1 and 0.01 respectively. And the hyperbolic negative sampling number  $n_{neg}$  is

<sup>7</sup>Although the HGCF reported the optimal layer number as 4, it ended up choosing 3 because they were almost identical.

<sup>8</sup>In practice, we found that if training epochs are enough, the effect of the layer number is negligible.

adjusted from 10 to 500. Compared to previous work that generally trained for 500 epochs [33, 48, 49], we extended the training to 1000 epochs because we found many methods had not yet converged. Additionally, consistent with prior work, we employed an early stopping strategy, meaning that training was stopped early if the NDCG@10 on the validation set did not improve for 100 consecutive epochs.

### C In-depth Ablation Study

In order to gain a deeper understanding of each component, we conducted a further analysis of the performance of different components on head items and tail items separately. In line with the work [48], the head and tail items are designated according to the 20/80 rule, which stipulates that items are ranked based on their degrees. The top 20% are designated as the head (denoted H20), whereas the remaining 80% are categorized as the tail (denoted T20). Tables 5 present the experimental results. Here, HS symbolizes our Hyperbolic negative Sampling, PI stands for Power law prior-based Initialization, HA represents Hyperbolic neighbor Aggregation, and GP signifies Gate fusion with Prior. Parenthetical values reflect the

improvement relative to the first row of the table. From the results, we have the following insights:

- The performance of HS for head items and tail items is not consistent across datasets (row 2 in Table 5), indicating that HS may have different effects on different types of items depending on the dataset characteristics. On the other hand, PI+HA generally shows a preference for improving tail items (row 3 in Table 5), suggesting that PI+HA can capture the long-tail distribution of items more effectively.
- PI+HA+HS (*i.e.*, HGCH, row 6 in Table 5) and PI+HA+HS+GP (*i.e.*, HGCH+, row 7 in Table 5) consistently achieve better performance for tail items across all datasets, demonstrating their ability to handle the long-tail problem in recommender systems. Notably, Amazon-Book obtains an impressive maximum improvement rate of 68.1% for tail items, which is much higher than the other datasets. This indicates that the hyperbolic space’s exponentially expanding capacity enables the model to focus more on tail items [48], while our proposals emphasize this characteristic further by refining the hyperbolic model’s structure and training.